Supplementary Material

Doubly ionized OCS bond rearrangement upon fragmentation - experiment and theory

Mahmoud Jarraya,[a,b,c] Måns Wallner,[d] Saida Ben Yaghlane,[b] Emelie Olsson,[d] Veronica Ideböhn,[d] Richard J. Squibb,[d] Jérôme Palaudoux,[c] Gunnar Nyman,[e] Muneerah Mogren Al-Mogren,[f] John H. D. Eland,[g,*] Raimund Feifel,[d,*] Majdi Hochlaf [a,*]

[a] Université Gustave Eiffel, COSYS/IMSE, 5 Bd Descartes, 77454, Champs Sur Marne, France

[b] LSAMA, Faculté des Sciences de Tunis, Université de Tunis El Manar, Tunis, 2092, Tunisie

[c] LCP-MR, Sorbonne Université – UMR7614, 75231 Paris Cedex 05, France

[d] Department of Physics, University of Gothenburg, 412 58 Gothenburg, Sweden

[e] Department of Chemistry and Molecular Biology, University of Gothenburg, Gothenburg, 405 30, Sweden

[f] Department of Chemistry, College of Sciences, King Saud University, PO Box 2455, Riyadh 11451, Saudi Arabia

[g] Department of Chemistry, Physical and Theoretical Chemistry Laboratory, Oxford University, Oxford, OX1 3QZ, UK

Table S1: Optimized structural parameters (R_i in bohr and θ in degree), harmonic frequencies (ω_i, in cm^{-1}) and zero point vibrational energies (ZPE, in cm^{-1}) and total energies (E, in Hartree) of the molecular species involved in this work as computed at the RCCSD(T)/aug-cc-pV(Q+d)Z level of theory.

	R_1	R_2	θ	ω_1	ω_2	ω_3	ω_4	ZPE	E
O (^3P_g)									-74.99493065
O^+ (^4S_u)									-74.49819755
C (^3P_g)									-37.78663526
C^+ (^2P_u)									-37.37490089
C^{2+} (^1S_g)									-36.48289644
S (^3P_g)									-397.6682818
S^+ (^4S_u)									-397.2911828
S^{2+} (^3P_g)									-396.4330943
CO ($X^1\Sigma^+$)	2.139			2159.33				1079.65	-113.1903709
CO^+ ($X^2\Sigma^+$)	2.113			2210.47				1105.22	-112.6761715
CO^{2+} ($X^3\Pi$)	2.353			1461.56				730.77	-111.6752489
CS ($X^1\Sigma^+$)	2.913			1279.47				639.724	-435.7239201
CS^+ ($X^2\Sigma^+$)	2.830			1376.32				688.148	-435.3077480
CS^{2+} ($X^3\Pi$)	3.034			1035.02				517.5	-434.5201976
SO ($X^3\Sigma^-$)	2.808			1154.97				577.475	-472.8595007
SO^+ ($X^2\Pi$)	2.701			1321.98				660.982	-472.4812456
SO^{2+} ($X^1\Sigma^+$)	2.627			1428.75				714.366	-471.7691414
OCS ($X^1\Sigma^+$)	2.190	2.961	180.0	2088.52	872.54	523.75	523.75	2004.24	-510.9766309
OCS^{2+} ($X^3\Sigma^-$)	2.112	3.388	180.0	2239.98	527.17	326.61	326.61	1710.16	-509.8749955
OCS^{2+} ($a^1\Delta$)	2.120	3.325	180.0	2150.31	530.60	362.35	306.82	1675.02	-509.8227512
COS^{2+} ($X^3\Sigma^-$)	2.288	3.172	180.0	1622.74	584.01	137.56	137.56	1240.92	-509.8030516
COS^{2+} ($a^1\Delta$)	2.304	3.125	180.0	1540.63	605.60	151.45	149.83	1223.74	-509.7515190
COS^{2+} ($1^1A''$)	2.576	3.734	53.92	1054.17	709.66	328.97		1046.39	-509.7299407
COS^{2+} ($1^5\Pi$)	2.369	3.040	180.0	1599.40	702.01	131.45	131.21	1216.29	-509.6369265

Table S2: Dissociation energies (E, eV) of COS^{2+} leading to $[SO+C]^{2+}$ fragments laying in the 30 - 40 eV with respect to OCS ($X^1\Sigma^+$). For SO^+ and SO^{2+}, we used the excitation energies from Refs. [1,2]. We also used the data in Table S1 and from Ref. [3].

	Dissociation channel	E
L_1	SO^+ ($X^2\Pi$) + C^+ (^2P_u)	30.396
L_2	SO^+ ($a^4\Pi$) + C^+ (^2P_u)	33.528
L_3	SO^+ ($A^2\Pi$) + C^+ (^2P_u)	34.205
L_4	SO^+ ($1^2\phi$) + C^+ (^2P_u)	35.094
L_5	SO^+ ($b^4\Sigma^-$) + C^+ (^2P_u)	35.117
L_6	SO^+ ($X^2\Pi$) + C^+ (^4P_g)	35.728
L_7	SO^+ ($C^2\Pi$) + C^+ (^2P_u)	36.044
L_8	SO^+ ($2^4\Pi$) + C^+ (^2P_u)	36.346
L_9	SO^+ ($1^2\Delta$) + C^+ (^2P_u)	36.394
L_{10}	SO^+ ($b^2\Sigma^-$) + C^+ (^2P_u)	36.569
L_{11}	SO^+ ($1^4\Delta$) + C^+ (^2P_u)	36.963
L_{12}	SO^+ ($2^2\Sigma^+$) + C^+ (^2P_u)	36.996
L_{13}	SO^+ ($4^2\Pi$) + C^+ (^2P_u)	37.347
L_{14}	SO^{2+} ($X^1\Sigma^+$) + C (^3P_g)	38.546
L_{15}	SO^+ ($a^4\Pi$) + C^+ (^4P_g)	38.860
L_{16}	SO^+ ($A^2\Pi$) + C^+ (^4P_g)	39.537
L_{17}	SO^+ ($X^2\Pi$) + C^+ (^2D_g)	39.686
L_{18}	SO^{2+} ($X^1\Sigma^+$) + C (^1D_g)	39.810

Table S3: Dissociation energies (E, eV) of COS^{2+} leading to $[CO+S]^{2+}$ fragments laying in the 27 - 40 eV with respect to OCS ($X^1\Sigma^+$). For CO^+, we used the excitation energies from Ref. [4]. We also used the data in Table S1 and from Ref. [3].

	Dissociation channel	E
L_1	CO^+ ($X^2\Sigma^+$) + S^+ (^4S_u)	27.425
L_2	CO^+ ($X^2\Sigma^+$) + S^+ (^2D_u)	29.267
L_3	CO^+ ($A^2\Pi$) + S^+ (^4S_u)	29.987
L_4	CO^+ ($X^2\Sigma^+$) + S^+ (^2P_u)	30.466
L_5	CO^+ ($A^2\Pi$) + S^+ (^2D_u)	31.829
L_6	CO^+ ($A^2\Pi$) + S^+ (^2P_u)	33.028
L_7	CO^+ ($B^2\Sigma^+$) + S^+ (^4S_u)	33.146
L_8	CO^+ ($a^4\Sigma^+$) + S^+ (^4S_u)	33.214
L_9	CO^+ ($1^4\Delta$) + S^+ (^4S_u)	34.194
L_{10}	CO^+ ($b^4\Pi$) + S^+ (^4S_u)	34.517
L_{11}	CO^+ ($1^4\Sigma^-$) + S^+ (^4S_u)	34.754
L_{12}	CO^+ ($B^2\Sigma^+$) + S^+ (^2D_u)	34.988
L_{13}	CO^+ ($a^4\Sigma^+$) + S^+ (^2D_u)	35.056
L_{14}	CO^+ ($C^2\Delta$) + S^+ (^4S_u)	35.239
L_{15}	CO^+ ($D^2\Pi$) + S^+ (^4S_u)	35.890
L_{16}	CO^+ ($1^4\Delta$) + S^+ (^2D_u)	36.036
L_{17}	CO^+ ($B^2\Sigma^+$) + S^+ (^2P_u)	36.187
L_{18}	CO^+ ($a^4\Sigma^+$) + S^+ (^2P_u)	36.255
L_{19}	CO^+ ($b^4\Pi$) + S^+ (^2D_u)	36.359
L_{20}	CO^+ ($1^4\Sigma^-$) + S^+ (^2D_u)	36.596
L_{21}	CO ($X^1\Sigma^+$) + S^{2+} (^3P_g)	36.780
L_{22}	CO^+ ($C^2\Delta$) + S^+ (^2D_u)	37.081
L_{23}	CO^+ ($1^4\Delta$) + S^+ (^2P_u)	37.235
L_{24}	CO^+ ($X^2\Sigma^+$) + S^+ (^4P_g)	37.269
L_{25}	CO^+ ($b^4\Pi$) + S^+ (^2P_u)	37.558
L_{26}	CO^+ ($D^2\Pi$) + S^+ (^2D_u)	37.732
L_{27}	CO^+ ($1^4\Sigma^-$) + S^+ (^2P_u)	37.795
L_{28}	CO ($X^1\Sigma^+$) + S^{2+} (^1D_g)	38.184
L_{29}	CO^+ ($C^2\Delta$) + S^+ (^2P_u)	38.280

L_{30}	CO^+ ($D^2\Pi$) + S^+ (^2P_u)	38.931
L_{31}	CO^+ ($X^2\Sigma^+$) + S^+ (^2D_g)	39.562
L_{32}	CO^+ ($A^2\Pi$) + S^+ (^4P_g)	39.831

Table S4: MRCI/aug-cc-pV(Q+d)Z double ionization energies (E, eV) of COS^{2+} quoted with respect to the energy at the equilibrium geometry of OCS ($X^1\Sigma^+$) (i.e. OCS angle = 180°, CO distance = 2.190 Bohr and CS distance = 2.961 Bohr).

Electronic state	E
$X^3\Sigma^-$	32.248
$a^1\Delta$	33.407
$b^1\Sigma^+$	34.260
$1^3\Pi$	35.340
$1^1\Pi$	35.634
$1^5\Pi$	36.724
$2^3\Pi$	37.514
$3^3\Pi$	38.255
$1^5\Sigma^-$	39.132
$2^1\Pi$	39.114
$1^1\Sigma^-$	39.232
$2^1\Pi$	39.275
$2^3\Sigma^-$	39.535
$1^3\Sigma^+$	39.371
$1^3\Delta$	39.510
$2^1\Delta$	39.755
$2^3\Sigma^+$	40.458

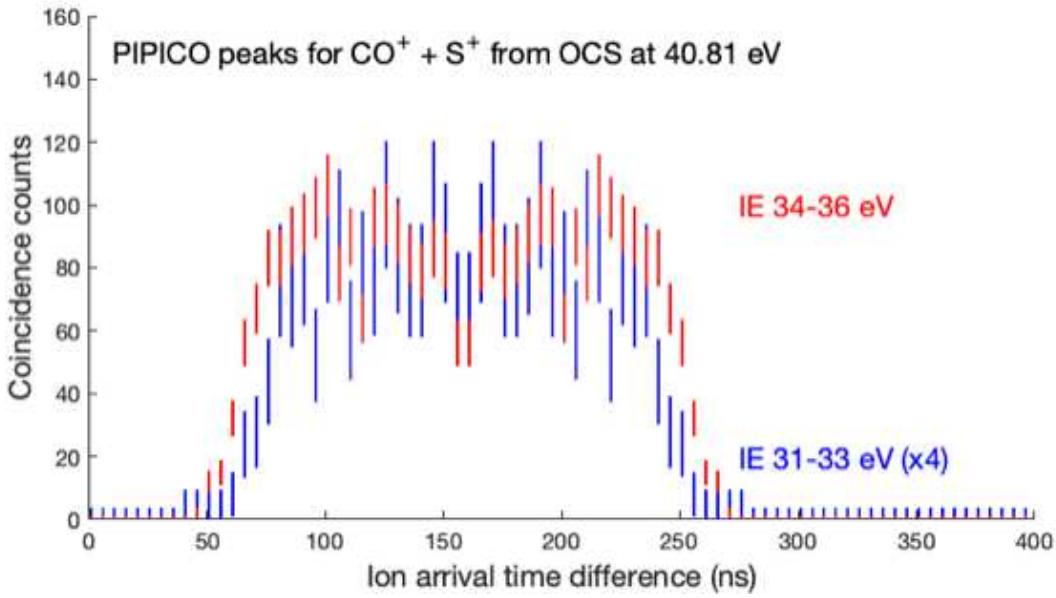

Figure S1: Arrival-time difference (PIPICO) peaks for CO^+ + S^+ ion pairs coincident with photoelectron pairs signaling double ionization in the energy ranges shown. The peaks have been artificially symmetrized about the time difference for thermal ions, using the later half of each raw PIPICO peak.

OCS^{2+} COS^{2+}

Figure S2: OCS^{2+} and COS^{2+} optimized structures and definition of their internal coordinates used for Table S1.

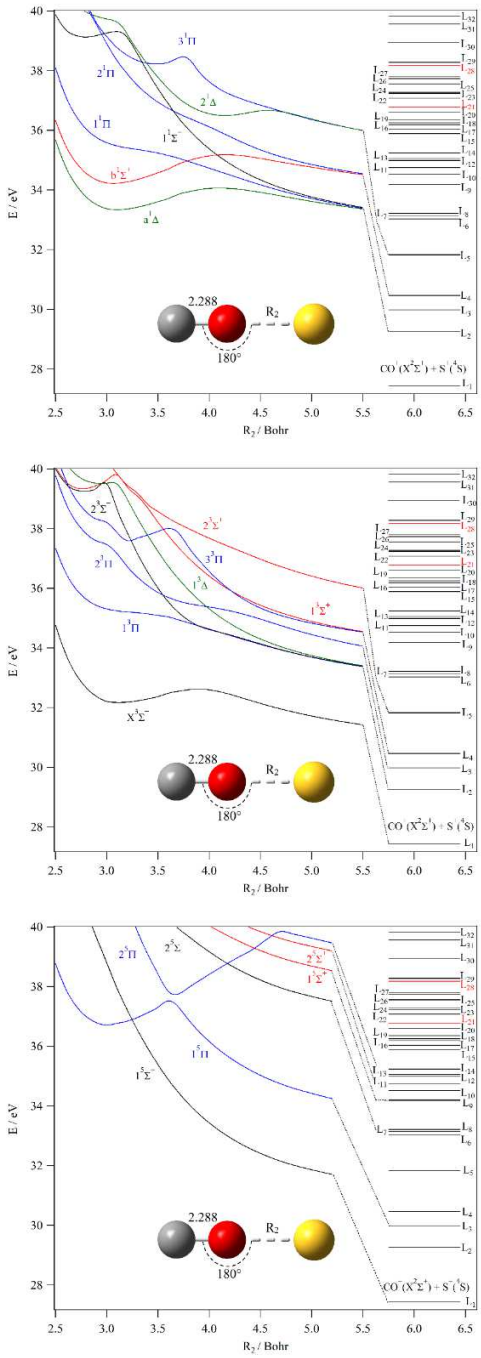

Figure S3: MRCI/aug-cc-pV(Q+d)Z potential energy curves of the singlet, triplet and quintet electronic states of COS^{2+} along the along the SO (R_2) coordinate. The remaining internal coordinates are kept fixed at their values in the COS^{2+} ($X^3\Sigma^-$) state i.e., R_1= 2.288 Bohr and θ= 180°.

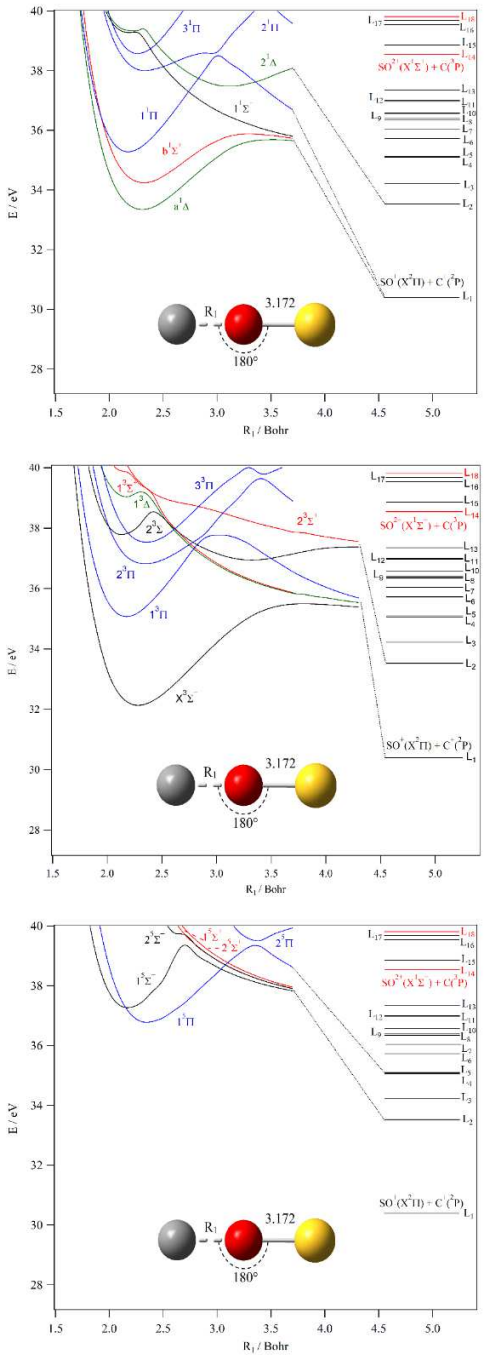

Figure S4: MRCI/aug-cc-pV(Q+d)Z potential energy curves of the singlet, triplet and quintet electronic states of COS^{2+} along the along the CO (R_1) coordinate. The remaining internal coordinates are kept fixed at their values in the COS^{2+} ($X^3\Sigma^-$) state (i.e., R_2= 3.172 Bohr and θ= 180°).

References

[1] A. Ben Houria, Z. Ben Lakhdar, M. Hochlaf, F. Kemp, and I. R. McNab. J. Chem. Phys. 122, 054303 (2005).
[2] A. Ben Houria, Z. Ben Lakhdar, and M. Hochlaf. J. Chem. Phys. 124, 054313 (2006).
[3] https://webbook.nist.gov
[4] D. Shi, W. Li, J. Sun, Z. Zhu, Y. Liu. Comput. Theor. Chem. 978, 126 (2011).